Erasmus University Rotterdam
Erasmus School of Economics
Master Thesis Quantitative Finance

Comparing EVT & Copula Network Models in European Banking

Bart Schrama (532580bs)

Supervisor:	Chen Zhou
Second assessor:	Phyllis Wan
Date final version:	8th August 2024

Abstract

This paper explores the interconnectedness between European banks using both the copula model and the extreme value theory model. Currently, stock market data is not utilized effectively in regulation, which could lead to significant improvements in accuracy and regulatory efficiency. By comparing full model copula graphs with tail-specific extremal graphs, this study enhances the understanding of banking networks. Using daily stock prices from January 2000 to April 2024 for 55 banks, the extremal model reveals a stronger relationship between G-SIB scores and centrality metrics, providing valuable insights into interconnectedness scores and capital surcharges. Moreover, the centrality-based analysis compares full and tail-based modelling methods, finding extremal models to be superior in graphical analysis, based on significance. Despite this, the models perform similarly during periods of economic stress, with the main differences in performance due to the model type rather than the measure used. In conclusion, the study suggests adopting extremal models for the potential integration of market data into Basel regulations.

Contents

1 Introduction

The Great Financial Crisis (GFC) of 2007-2008 and more recent bank failures such as First Republic Bank (2023) have reiterated the importance of robust financial systems. The GFC led to the collapse of major financial institutions, massive bailouts, and a significant downturn in global economic activity. More recently, bank failures have continued to threaten financial stability (e.g. Silicon Valley Bank), underlining the critical need for resilient financial systems. A single bank failure can pose a significant risk to the entire financial system and the global economy. For banks deemed "too big to fail", failure may even result in government-supported bailouts ultimately funded by taxpayers (Rosas, 2006; Stiglitz, 2009). To accurately assess the importance of banks and their roles within the financial system, the Basel Committee has introduced comprehensive models and extensive legislation to recapitalize banks and impose stronger capital requirements on key institutions.(Rubio & Carrasco-Gallego, 2016). Consequently, new models must be consistently pioneered to ensure that regulations remain efficient and effective.

The systemic importance of banks can stem from various characteristics. The Basel Committee builds on five categories: size, interconnectedness, substitutability, complexity, and cross-jurisdictional activity. Size has been thoroughly discussed in Zhou (2010), finding that size should not be considered a direct proxy and that the too-big-to-fail argument does not always hold. However, large banks with diversified banking activities might become systemically important, tying into the case for complexity and the findings in Carmassi and Herring (2016) on globally systemically important banks (G-SIBs). Substitutability carries relatively little weight as discussed in Allahrakha, Glasserman and Young (2015), leaving the cross-jurisdictional and interconnectedness scores as the primary categories to consider. Busch, Cappelletti, Marincas, Meller and Wildmann (2021) show that there is a lot to gain in these topics as the current G-SIB framework uses only balance sheet information, omitting market data. This opens up significant opportunities to strengthen the identification of key banks, particularly within the interconnectedness category, by using direct market relations. Building on this, we introduce extremal models, compare them with existing copula models, and evaluate the initial effectiveness of the methodology in integrating market data into Basel regulations.

Understanding the connectedness between institutions remains crucial for effectively preventing or handling financial crises. Underestimating risks or incorrectly identifying key banks could lead to failures due to insufficient capital requirements, while overly capitalizing banks could result in unproductiveness and reduced international competitiveness. Furthermore, Engle, Jondeau and Rockinger (2014) find that their measure of systemic risk directly Granger-causes industrial production and business confidence indices, signalling distress in economies and the significant importance of a strong financial system. Additionally, banks designated as G-SIBs capitalize on better debt guarantees and sig-

nificantly higher implicit guarantee values compared to non-G-SIBs (Schich & Toader, 2017) suggesting a direct impact of the assigned scores.

Identifying key institutions that are subject to higher contagion or whose failure could cause a further breakdown in the system is thus central to this framework. Overall, this research will benefit regulators by contributing to the literature on interbank relations. Possibly contributing to the open problem that is the continuing development of Basel IV.

The current literature on the interconnectedness problem already uses network models to help identify key relationships. For example, Cerchiello and Giudici (2016) plot directional risk relations, aiming to visualise the discussed interconnectedness using market data. However, because most systemic risk is concentrated during economic crises and regulatory overhauls, research may benefit from shifting from a general approach to a more tail-centric focus. For example, Baumöhl, Bouri, Hoang, Shahzad and Výrost (2022) focus on tail dependence.

The tail has also been explored in the works of Z. Zhang, Zhang, Wu and Ji (2021) and Denkowska and Wanat (2020), which use copula models to take the tail into account. Unfortunately, the copula methodology still requires us to model the entire distribution. An even more targeted methodology may thus be applied, using extreme value theory to model the tail itself. Thus, to further explore interbank relationships and the impact of events on these relationships, this study investigates how copula-based and EVT (Extreme Value Theory) based graphical models compare in identifying and evaluating the systemic importance of banks. Specifically, the study examines the centrality of banks in these models and their effectiveness in capturing interbank dependencies under various market conditions. The tail model should, in theory, be less influenced by general observations, allowing for stronger results in non-crisis periods and increased accuracy of the inferences. Consequently, during crisis periods, the models should exhibit higher levels of similarity as the data used becomes more uniform.

The models utilize daily stock prices retrieved from Refinitiv Eikon for STOXX600 banks, along with macroeconomic indicators from Eurostat and the Office of Financial Research. Because stock prices are forward-looking, they have significant predictive power for potential financial distress. Europe is selected for its diversity of countries, allowing unique clusterings under the same regulatory framework.

Using the Copula and EVT methodologies, graphs are fit for the last five years showing interpretations of the European framework. In addition, a time series of graphs spanning January 2000 up to April 2024 is used to explore graphical implications through centrality measures and to identify the relationship between the models. By examining the centrality of banks in the individual models and the rank correlation between the centrality measures across the models it is found that: Firstly, EVT-based centrality scores seem to be far more effective at explaining bank importance compared to the copula-based scores. This

is likely due to a stronger focus on extremes rather than general observations, which are dominated by local market effects. Secondly, the rank correlation between the graphs seems influenced by economic conditions, rising significantly in bear markets and crises. Lastly, a change in trend is observed around the Brexit negotiations, after which increased market volatility and more extreme observations potentially diluted the effect of normal non-important observations in the copula models. Moreover, the Brexit effect also appears in visual inspections of the graphs as the British banks move towards the outer regions of the graphs. Ultimately, the study finds that the EVT model is better at classifying G-SIBs and, potentially, aiding in effective regulation.

Hence, these results also have policy implications. regulators should be aware of the differences between the models and the results produced by the different methodologies. Using the copula model could yield less relevant results, limiting the effectiveness of possible further regulation on the identified banks. Moreover, the results highlight that the system remains vulnerable to large-scale events which can greatly affect the dependence structures among banks. This suggests that after key events the interconnectedness needs to be thoroughly reevaluated, as banks may shift in positions and thus in regulatory importance.

The remainder of the paper is divided into the following sections. Section 2 provides background on graphical modelling theory and overviews the extreme value interpretation of the graphical model as pioneered by Engelke and Hitz (2020). Section 3 covers the data and data processing for the stock prices and macroeconomic data used. Section 4 discusses the practical implementation of the theory and the estimation of the models. Section 5 presents the results and their implications, followed by the conclusion in Section 6.

2 Theoretical Framework & Background

2.1 Graphical Models

Graph theory is a popular choice for models that require the user to describe or understand the interactions between a large set of random variables (Yang & Peng, 2020). Graphical models have since been used to infer networks and model problems on interconnected entities, for example with graphical LASSO (Hallac, Park, Boyd & Leskovec, 2017). Similarly, network analysis has been directly applied to stock markets as in Huang, Zhuang and Yao (2009), who model the topological changes in the network to infer correlation patterns and guide risk management. Using their correlation threshold method they create networks to study the relationship between network characteristics and correlation thresholds. Furthermore, graphical models can be used to predict stock prices such as in Li et al. (2021) and Yin, Yan, Almudaifer, Yan and Zhou (2021).

A specific subset of graphical models aims at building minimum spanning trees (MST),

a subsection of connected graphs without cycles, which minimize the total weight of the edges. These Non-directional connected tree models are often created using Prim's Algorithm (Prim, 1957) as it finds the minimum spanning tree in weighted, undirected graphs. In this paper's application, the algorithm uses weights denoted in a matrix to compare the length of the edges. For this distance matrix, many methods have also been used. Often, stock market analysis has been done using MSTs based on correlation matrices, for example, for the Italian market (Coletti, 2016) and the Polish market (Tomeczek, 2022). Moving past correlation matrices, Millington and Niranjan (2021) used rank correlation and Baumöhl et al. (2022) consider the tail of the distribution. Baumöhl et al. specifically introduced a directed model, allowing them to measure whether the institution is a net risk transmitter or receiver; moreover, they can do so for quantiles of the distribution, all the way up to 5%.

Moving further into the tail there are the copula models. Ranging from those developed for exchange rates (Wang, Xie, Zhang, Han & Chen, 2014), the Chinese Financial Market (Z. Zhang et al., 2021), to the European Insurance Market (Denkowska & Wanat, 2020). These copula papers base their dependency measure on Spearman's rho, a rank correlation, which can be calculated using the mathematical definition of different copulas. By doing so, the authors are able to fit various copulas with different tail dependencies to the data and get various fits for the chosen correlation parameter. Notably, Z. Zhang et al. (2021) also use time-varying copula parameters to achieve similar results. After selecting their copulas, the authors select an information criterion optimal copula to make their graph. While this method also accounts for tail dependence, it is still affected by regular observations, and for some copulas even significantly by the right tail of the return distribution due to symmetry assumptions.

With the key focus of modelling risks in the network, it makes more sense to move towards left tail-focused methods that only take into account extreme distress scenarios when graphing financial interdependency. To this extent, there are either extreme value copulas (Ribatet & Mohammed, 2013) as intermediaries, or extremal graphs based on papers from Engelke and Hitz (2020), focusing on tree creation based on extremal coefficients. The following section reviews the literature on applying extreme value theory to graphs.

2.2 Extreme Value Theory

2.2.1 Multivariate Pareto Distributions

The multivariate Pareto distribution is introduced in Rootzen and Tajvidi (2006). They base their interpretation on the peak-over-threshold model and formalize a generalized multivariate Pareto distribution.

Subsequently, Engelke and Volgushev (2022) build on this by defining multivariate

exceedances for the vector $\mathbf{X}$ as any observation where at least one component of $\mathbf{X}$ exceeds its quantile. In our case $\mathbf{X}$ represents the processed returns of all banks on a certain day, with bank $i \in V$ for V the set of banks, with the corresponding cumulative distribution function $F(\mathbf{x}) = (F_1(x_1), ..., F_d(x_d))$ of $\mathbf{X}$. The multivariate Pareto distribution is shown in equation 1, for some vector $\mathbf{Y}$ supported on $\mathcal{L} = \{\boldsymbol{x} \geq \mathbf{0} : \|\boldsymbol{x}\|_\infty > 1\}$ for all points $\boldsymbol{x} \in \mathcal{L}$. Note that $F(\boldsymbol{X}) \not\leq 1 - q$ shows that at least one observation in $\boldsymbol{X}$ is exceeding the marginal quantile of $F_i^{-1}(1-q), i \in V$. In other words, this takes the limit over all observations for $\boldsymbol{X}$ where at least one X_j is an extreme value.

$$\mathbb{P}(\boldsymbol{Y} \leq \boldsymbol{x}) = \lim_{q \to 0} \mathbb{P}(F(\boldsymbol{X}) \leq 1 - q/\boldsymbol{x} \mid F(\boldsymbol{X}) \not\leq 1 - q), \tag{1}$$

Engelke and Volgushev (2022) show that the random vector of returns $\boldsymbol{Y}$ has homogeneity as a structural property, linking it to the univariate Pareto distribution as $\mathbb{P}(\boldsymbol{Y} \in tA) = t^{-}1\mathbb{P}(\boldsymbol{Y} \in A)$ for any transformation $tA = \{tx : x \in A\}$ for subsets $A \subset \mathcal{L}$ implying that for all $i \in V$ it can be shown that $\mathbb{P}(Y_i \leq x | Y_i > 1) = 1 - 1/x, x \geq 1$. in other words, $Y_i | Y_i > 1 \sim Pareto$.

2.2.2 Conditional Independence

Because the above multivariate Pareto distribution is not defined across the entire space of $\mathbf{X}$ an auxiliary vector needs to be derived to create a non-standard form of conditional independence. Hence, for any $m \in V$ we denote $\mathbf{Y}^m := \mathbf{Y} | \mathbf{Y}^m > 1$ on support space $\mathcal{L}^m = \{x \in \mathcal{L} : x_m > 1\}$.

Based on the multivariate Pareto distribution, Engelke and Volgushev (2022) define a general conditional independence for extreme observations. For the index set V of graph $G = (V, E)$ over the extreme observations described by a multivariate Pareto distribution $\mathbf{Y}$ with the disjoint sets $A, B, C \subset V$, then $\mathbf{Y}_A$ is conditionally independent of $\mathbf{Y}_C$ given $\mathbf{Y}_B$ if there is no path between A, C without a node from B.

$$\forall m \in \{1, ..., d\} : \quad \mathbf{Y}_A^m \perp\!\!\!\perp \mathbf{Y}_C^m | \mathbf{Y}_B^m \tag{2}$$

Also denoted as: $\mathbf{Y}_A \perp_e \mathbf{Y}_C | \mathbf{Y}_B$ where subscript e indicates it is defined for extreme observations. Note that the implied pairwise Markov property is equivalent to the global Markov property for the graph G as long as it is connected. Under the assumption of an auxiliary random vectors derived from $\mathbf{Y}$ the conditional independence does not assume densities, making it more general than the one described in Engelke and Hitz (2020).

2.2.3 Extremal Correlation & Extremal Variogram

The extremal equivalent of the covariance matrices used in the Gaussian model could be the extremal correlation (Equation 3). Defined for $i, j \in V$ the extremal correlation meas-

ures the strength of dependence in the extremes of variables. The extremal correlation is bounded by 0 and 1, with independence and complete extremal dependence at its limits (Coles, Heffernan & Tawn, 1999). Moreover, if $\mathbf{X}$ is in the max-domain of attraction of the multivariate Pareto distribution $\mathbf{Y}$ then the extremal correlation always exists.

$$\chi_{ij} := \lim_{q \to 0} \mathbb{P}\left(F_i(X_i) > 1 - q | F_j(X_j) > 1 - q\right) \tag{3}$$

However, the extremal variogram may be even better positioned to compare as an extremal covariance. This extremal variogram can be interpreted as shown in equation 4. Implying that $\Gamma_{ij}^{(m)}$ is large if the extremal dependence is weak between bank i and j, and small when the extremal dependence is large. Note that the extremal variogram is rooted at a node $m \in V$ yet has a clear link to the extremal correlation χ_{ij} which is not rooted.

$$\Gamma_{ij}^{(m)} = \mathrm{Var}\left(\log Y_i^m - \log Y_j^m\right) \tag{4}$$

The exact relation between the extremal correlation and extremal variogram depends on the assumed distribution of the extremal functions $\mathbf{W^1}, ..., \mathbf{W^d}$ that uniquely define the distribution of $\mathbf{Y}$. With extremal function W_i^m, rooted at node m for bank i. Where $\mathbf{Y^m} =^{(d)} P\mathbf{W^m}$ for some Pareto random variable P and $\mathbf{W_m^m} = 1$.

The Hüsler–Reiss distribution (Hüsler & Reiss, 1989), which is parametrised by the variogram matrix of Γ, is selected because of a special property. Namely, Engelke and Hitz (2020) show that the extremal variogram $\Gamma^{(m)}$, rooted at m, is equivalent to the variogram matrix Γ for $\forall m \in V$. Because of this an exact relation can be made between the extremal correlation and extremal variogram as denoted in Equation 5. Note that the variogram matrix Γ is a symmetric conditionally negative definite matrix, closely related to the covariance matrix through the relation $\Gamma_{ij} = \mathbb{E}(Z_i - Z_j)^2 = \Sigma_{ii} + \Sigma_{jj} - 2\Sigma_{ij}$ for banks i, j for some random vector $\mathbf{Z}$ with covariance matrix Σ. However, multiple covariance matrices may correspond to a single Γ (Farris, Kluge & Eckardt, 1970). The remainder of this paper assumes the Hüsler–Reiss distribution, meaning that the below formula holds.

$$\chi_{ij} = 2 - 2\Phi(\Gamma_{ij}/2) \tag{5}$$

3 Data

The dataset is based on stock price observations retrieved from Refinitiv Eikon[1] and consists of the daily price observations for all constituents of the STOXX600 Banks index (EXV1). Additionally, UBS, Morgan Stanley, Goldman Sachs, Wells Fargo, Citi, and JP. Morgan were added to the dataset, resulting in 55 banks with observations from 1st

[1]Retrieved April 2nd 2024

January 2000 to 2nd April 2024. As some banks have not publicly traded for some period the dataset starts with 40 banks, see Appendix 8 for an overview. Table 1 shows descriptive statistics for the European banks, here the average market cap is at 25 €bn with the smallest bank at 2.3 €bn compared to the largest at 137 €bn+. Implying significant differences across the banks in the sample. While similar differences appear in the other statistics, the ratios between net interest income and revenue and net income and revenue appear relatively stable. A full overview of the banks can be found in Appendix Table 5 with Appendix Figure 9 showing the rebased prices for selected banks. Notably, the banks follow similar patterns, with BNP Paribas generally pricing above the others. Overall the movements are similar across the banks and, as expected, in line with the STOXX600 Banks Index.

Table 1: Descriptive statistics for European banks. Shows Market Capitalization, Net Total Loans, Net Income, Total Revenues, and Net Interest Income (NII) in millions.

€mm	**Market Cap**	**Total Loans**	**Net Income**	**Revenue**	**NII**
Average	25,571	272,560	4,060	13,193	7,719
Median	17,203	181,909	2,577	6,200	4,487
Min	2,311	1,997	163	384	138
25%	6,195	56,804	950	3,367	2,525
75%	32,420	448,802	4,934	19,744	10,212
Max	137,566	1,094,266	25,775	60,546	43,261

Despite the daily fluctuations that are not related to the underlying, stock prices remain the best widely available proxy for bank performance and financial risk, as also indicated in Z. Zhang et al. (2021) for the Chinese Financial Market, Denkowska and Wanat (2020) for the European insurance market, and van Oordt and Zhou (2019) for systemic risk modelling in banks.

To transform the stock data we take the difference of the logs to get the log returns, see Equation 6 for day t and bank i. The returns are negated to get the log losses.

$$r_{i,t} = \log(p_{i,t}) - \log(p_{i,t-1}) \tag{6}$$

After transforming to log-losses, various ARMA-GARCH models are individually fit to all banks. The ARCH methodology is based on Bollerslev, Chou and Kroner (1992) and the ARMA-GARCH specification is selected based on the average Akaike Information Criterion (AIC) across the set of banks, as done in Engelke and Volgushev (2022). Based on the average AIC the ARMA(0,2)-GARCH(1,1) model (see Equation 7) is selected. After selecting the model the residuals are obtained for each bank cleaned of their serial dependence.

$$
\begin{aligned}
r_{i,t} &= \varphi_0 + \varepsilon_{i,t} + \theta_1 \varepsilon_{i,t-1} + \theta_2 \varepsilon_{i,t-2}, \\
\sigma^2_{i,t} &= \alpha_0 + \alpha_1 \varepsilon^2_{i,t-1} + \beta_1 \sigma^2_{i,t-1}, \\
\varepsilon_{i,t} &= \sigma_{i,t} z_{i,t}, \quad z_{i,t} \sim N(0,1)
\end{aligned} \tag{7}
$$

To evaluate the current state of the European banking system the last 5 years are selected. Then, to extend past the visual comparisons, we employ a rolling window estimation method with a three-year interval. This involves segmenting the dataset into overlapping windows, yielding a total of 256 observations. The end dates of these windows are updated monthly, starting from December 2002 and continuing through to December 2023. This approach enables us to capture the evolving nature of the relationships over time.

In addition to the stock market data for the banks, seasonally adjusted quarterly GDP growth data from Eurostat (2024) is included. Furthermore, the Financial Stress Index (FSI) and the European-Japanese Financial Stress Index (EUJP) provided by Office of Financial Research (2024) are included along with the G-SIB scores for individual banks. For the G-SIB data we only consider the European banks resulting in 114 observations split across time between 2014 and 2023, consisting of 13 different banks.

The OFR FSI was selected because it has a direct relation with decreases in economic activity, performing well in identifying systemic financial stress scenarios (Monin, 2019). Similarly, GDP growth acts as a proxy for the macroeconomy, which has been found to influence systemic risk levels through the herd-like behaviour of banks (Calmès & Théoret, 2014).

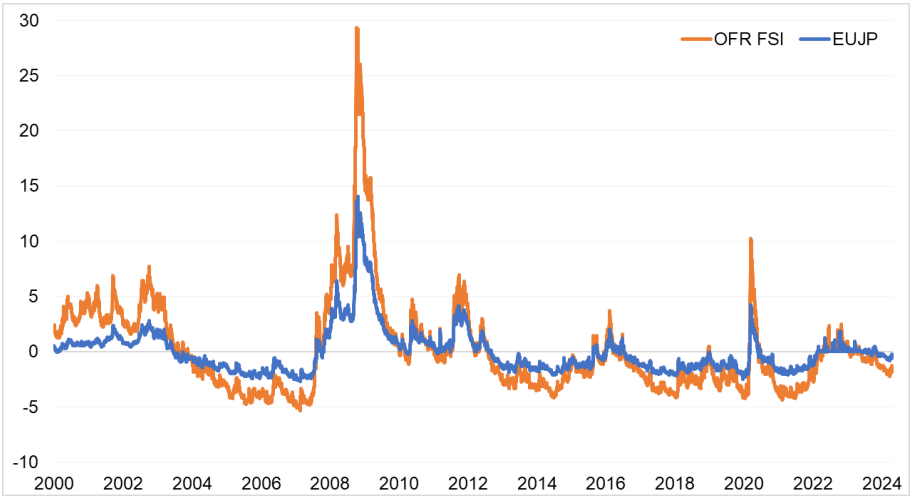

Figure 1: Plot of OFR Financial Stress Index (FSI) and European Japanese subdivision of the financial strength index. This figure shows the period 2000 to 2024 for the stress indicator

As shown in Figure 1, the FSI has moved significantly over the last 20 years, with large spikes during the Great Financial Crisis, the Eurocrisis, and the pandemic. Overall, the European-Japanese subsection seems to have followed similar patterns but with less

extreme fluctuations. Furthermore, the quarterly GDP shown in Appendix Figure 10 exhibits similar movements, with quarterly decreases around the crisis periods, going negative after the GFC, during the Eurocrisis, and in the pandemic.

4 Methodology

Using the processed data we need to estimate the relevant distance matrices for Prim's algorithm to create the minimum spanning tree (MST) (Prim, 1957). Prim's algorithm is a greedy algorithm that iteratively adds the closest vertex. This way the algorithm always produces a tree $G = (V, E)$ with the set of vertices V, corresponding to the banks, and the edges E, as $|E| = |V| - 1$. Hence, for some set of symmetric weights (distances) $d_{ij} > 0$ associated with vertices $i, j \in V, i \neq j$ the tree is given by Equation 8.

$$T_{mst} = \underset{G=(V,E)}{\operatorname{argmin}} \sum_{(i,j)\in E} d_{ij} \tag{8}$$

The input for Prim's algorithm can come from various models, with the key distinction being between full models and tail models. Specifically, the focus will be on the full model in the copula form, as discussed in Section 4.1, and the tail model, discussed in Section 4.2. Table 2 shows that besides the model type there is also the difference in measure. Note that while modelling a full measure from a tail model is not possible, we can use a full model to say something about the tail. Appendix A highlights this for the copula-specific interpretation.

Table 2: This table compares the full and tail-based modelling methodologies, along with the corresponding full and tail-based measures used in combination with the models. A full model can provide both a full measure and a tail measure, while a tail model can only provide a tail measure.

		Model	
		Full	Tail
Measure	Full	Section 4.1	X
	Tail	Appendix A	Section 4.2

4.1 Copula-Based Graphs

For the copula method we choose to use the empirical CDF over the skewed Student-t marginals (Hansen, 1994) opposed to what was suggested by previous work from Z. Zhang et al. (2021) stating its ability of addressing skewness, kurtosis, and fat-tails remaining in the residuals. Nevertheless, in the current implementation there are no key advantages of fitting a specific parametric marginal over an empiric CDF. All copulas are fit based on

the pairwise matching of the empirical Kendall's Tau. In general, we have the copula in Equation 9 for the processed stock prices x, y of banks X, Y.

$$F_{XY}(x, y) = C\left(F_X(x), F_Y(y)\right). \tag{9}$$

Two different copulas are compared, namely the Gumbel Copula and the Frank Copula, denoted by equations 10 and 11, respectively:

$$C_{\mathrm{Gu}}(x, y; \delta) = \exp\left(-\left((-\log x)^{\delta} + (-\log y)^{\delta}\right)^{\frac{1}{\delta}}\right) \tag{10}$$

$$C_{\mathrm{Fr}}(x, y; \theta) = -\frac{1}{\theta}\ln\left[1 + \frac{\left(e^{-\theta_x} - 1\right)\left(e^{-\theta_y} - 1\right)}{e^{-\theta} - 1}\right] \tag{11}$$

After fitting the copulas we calculate the pairwise Spearman's Rho for each combination using Equation 12, for copula function $C(x, y; \theta)$ representing the fitted copula between bank X and bank Y. After calculating the Spearman's rho we calculate the distance measure $d_{XY} = \sqrt{2(1 - \rho_{XY}^{SP})}$.

$$\rho_{XY}^{SP} = 12\int_0^1\int_0^1 C(x, y; \theta)dxdy - 3, \tag{12}$$

4.2 Extremal Trees

The extremal trees are based on the empirical variogram and the background methodology explored in section 2.2. Using the same processed residuals as for the copulas, we denote X_{ti} for daily observations at time t for the banks $i \in 1..d$. The empirical variogram is defined in Equation 13, where $\tilde{F}_i(.)$ is the empirical CDF of some X_i and k is the number of exceedances selected. Note that this is the elementwise calculation of the extremal variogram rooted at m. Moreover, the $\hat{Var}$ denotes the sample variance and $k/n \to q$ for $n \to \infty$.

$$\hat{\Gamma}_{ij}^{m} := \hat{Var}\left(\log(1 - \tilde{F}_i(X_{ti})) - \log(1 - \tilde{F}_i(X_{tj}) : \tilde{F}_m(X_{tm}) \geq 1 - k/n\right) \tag{13}$$

Engelke and Volgushev (2022) show that if the right side of the equation exists then the underlying extremal conditional independence tree can be consistently recovered. Furthermore, under the assumption of Hüsler–Reiss distributions the root node is irrelevant.

The variogram is then converted to the extremal correlation coefficient using the element-wise relation $\chi_{ij} = 2 - 2\Phi(\sqrt{\Gamma_{ij}}/2)$. The Prim algorithm is then used on the weights $d_{ij} = 2 - \chi_{ij} \in [1, 2]$ where high extremal correlations (implying small variograms) result in a smaller distance. This method is used over the direct empirical extremal correlation because the extremal variogram is, in theory, guaranteed to recover the underlying

tree as long as all variograms exist.

The number of exceedances k is set according to the methodology of Engelke and Volgushev (2022), extended slightly for the smaller moving windows.

4.3 Centrality Measures

To assess the created graphs and provide a basis for comparison we need descriptive measures of the graphs. To this extent, Z. Zhang et al. (2021) measure centrality and density in the network by using measures derived from Spearman's Rho's moments. As this is not universally applicable between our methods, we use topological measures for centrality (Wang et al., 2014; Tomeczek, 2022). We use three centrality measures, namely closeness, betweenness, and degree centrality. (J. Zhang & Luo, 2017)

Closeness centrality, as shown in Equation 14, measures the shortest distance of bank v (vertex $v \in V$) to all other banks (vertices) in the graph. $d(\cdot, \cdot)$ is the distance function and $n-1$ is a normalization term, for n banks in the graph, allowing us to compare different sized graphs.

$$C_c(v) = \frac{n-1}{\sum_{u \neq v} d(v,u)}, \tag{14}$$

Similarly, we define (vertex) betweenness centrality as shown in Equation 15. (Freeman, 1978) This measures the number of times a bank (v) is bridged by the shortest path between two other banks ($s, t \in V$). σ_{st} is the total number of shortest paths between s and t, while $\sigma_{st(v)}$ is the number of shortest paths that go through bank v. The term $\frac{2}{(n-1)(n-2)}$ is a normalization term.

$$C_b(v) = \sum_{s \neq v \neq t} \frac{\sigma_{st}(v)}{\sigma_{st}} \frac{2}{(n-1)(n-2)} \tag{15}$$

Lastly, degree centrality, shown in Equation 16, is calculated which corresponds to the number of links a bank v has to other banks. Note that we again normalize by $n-1$ to compare different sized graphs.

$$C_d(v) = \frac{\deg(v)}{n-1} \tag{16}$$

Using the centrality scores for the individual banks we can check the G-SIB specification assigned by the Basel Committee. We check the overall Systemic Importance Score (SIS) and the Interconnectedness scores by means of individual regressions for each centrality measure, see Equation 17 and 18, respectively. In these formulae the C_{it} variable refers to one of the three centrality measures ($i = (c, b, d)$) for the graph ending in period t. The regression only includes observations for European network banks as the American network is underdeveloped and underrepresented in our dataset. After this restriction this

leaves 114 observations.

$$SIS_t = \beta_0 + \beta_1 C_{it} + \varepsilon_t \tag{17}$$

$$Int_t = \beta_0 + \beta_1 C_{it} + \varepsilon_t \tag{18}$$

4.4 Rank Correlation

To effectively measure the similarity between the graphs produced by various methods, we introduce rank correlation as a new statistic. The rank correlation can be calculated using the previously computed centrality measures for the extremal and copula graphs. A time series is created by calculating the correlation over time using a 1-month rolling window with a length of 3 years. The rank correlation is computed with the calculated centrality measures using Equation 19 for Spearman's rho, where l_i is the difference in rank for some bank i between the copula and extremal trees.

$$\rho_{\text{Spearman}} = 1 - \frac{6 \sum l_i^2}{n(n^2 - 1)} \tag{19}$$

After calculating the rank correlation we perform tests on the time series. First we test for stationarity using the Augmented Dickey-Fuller framework. The first test is shown in Equation 20. For rank correlation RC_t in period t we assume no drift and have a null hypothesis of non-stationarity, namely $\gamma = 0$. Note, the optimal lag number (p) is selected using the BIC criterion.

$$\Delta RC_t = \gamma RC_{t-1} + \delta_1 \Delta RC_{t-1} + \delta_2 \Delta RC_{t-2} + \ldots + \delta_p \Delta RC_{t-p} + \varepsilon_t \tag{20}$$

After finding that the null hypothesis is not rejected (at 5%) and that the unit root might be present the second test in Equation 21 is performed. Here we test the null hypothesis of $\gamma = 0$ and the null hypothesis of $\alpha = \gamma = 0$. At both the 1% and 5% level both null hypotheses are rejected, implying that the unit root is not present and there is a drift.

$$\Delta RC_t = \alpha + \gamma RC_{t-1} + \delta_1 \Delta RC_{t-1} + \delta_2 \Delta RC_{t-2} + \ldots + \delta_p \Delta RC_{t-p} + \varepsilon_t \tag{21}$$

Furthermore, using three regressions the movements in the rank correlation are tested. Equation 22 shows the GDP regression, Equation 23 and 24 show versions of the financial stress index (FSI), and Equation 25 shows the multiple regression of all features. In all equations we have the rank correlation RC_t for that period t regressed on a constant β_0 and the dependent variable, assuming normal errors. We include the date variable t to

adjust for the aforementioned drift, as suggested by Childers (2024).

$$RC_t = \beta_0 + \beta_1 GDPG_t + \beta_2 t + \varepsilon_t \tag{22}$$

$$RC_t = \beta_0 + \beta_1 FSI + \beta_2 t + \varepsilon_t \tag{23}$$

$$RC_t = \beta_0 + \beta_1 EUJP + \beta_2 t + \varepsilon_t \tag{24}$$

$$RC_t = \beta_0 + \beta_1 GDPG_t + \beta_2 FSI + \beta_3 t + \varepsilon_t \tag{25}$$

The drift in the rank correlation is further investigated using subsequent F-tests to find potential structural breaks. This is an extension of the Chow test and uses the framework from Zeileis, Kleiber, Krämer and Hornik (2003). We perform this test for both the drift only regression as well as the regressions shown in Equation 22 and 23.

5 Empirical Results

5.1 Comparing Trees

Figure 2 and 3 show the minimum spanning trees created for the last 5 years based on the daily stock prices. In both graphs the countries appear similarly split, clustering around each other. However, the extremal tree moves UBS closer to the centre around Société Générale, in contrast to the link with the German banks found in the Copula version. Figure 3 also links the British banks through the German and Spanish banks, in contrast to the direct link with Crédit Agricole in the Copula tree.

The EVT graph identifies CAGR, BNP, SOGN, ISP, SAN, DBKGn, INGA, RBIV, and NDASE as the most important banks in the European System, while in the more spread out Copula tree we do not identify RBIV. Notably the Copula tree does identify ABN Amro as a potentially important bank as it links closely to the USA, however this is most likely due to a relatively large share of the non-local revenue coming from the US branch compared to the rest of Europe[2]. This may indicate that the copula based model puts more importance on low-level information retrieved from daily market movements of the American exchanges, opposed to risk-driven changes. Note that the results for the Frank copula are identical to the Gumbel Copula (see Appendix C).

[2]2023 Profit is distributed as 2,290mm in the Netherlands, 101mm in rest of Europe, 207mm in the USA, and 97mm in rest of the world.

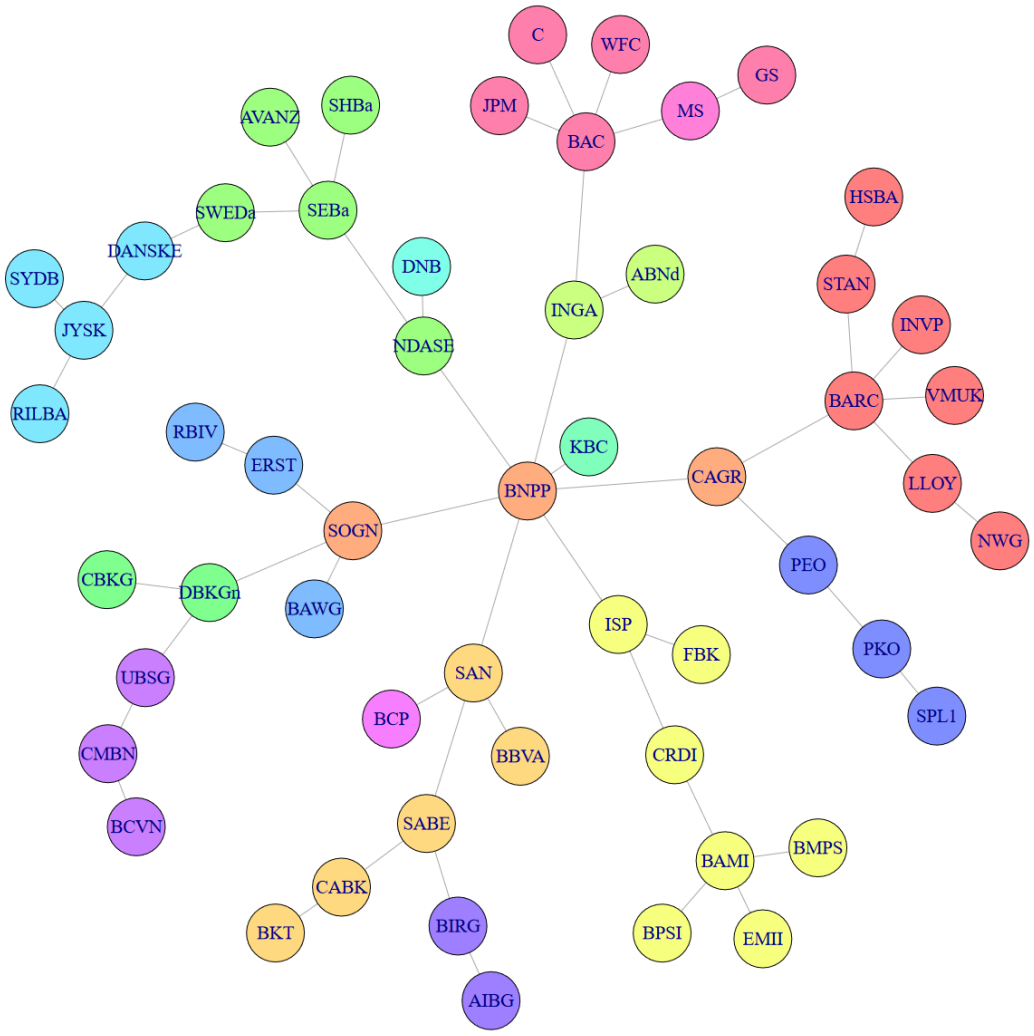

Figure 2: Network structure of European banks based on the Gumbel copula. Based on last 5 years of data from April 2019 to April 2024. Bank indices are in Appendix Table 5

5.2 Centrality Driven Results

In addition to the graphical movements, we measure the centrality and relative importance of the banks in the network. Table 3 shows a significant link between the centrality of a bank and the bank's G-SIB score and subsequent capital surcharges. Next to verifying the accuracy this implies that graphical location may be a suitable determinant to add or remove additional charges. For example, based on the previous last 5 year graph, Deutsche Bank appears to be too strongly regulated based on its graphical importance while ISP might need stronger capital requirements.

Table 3 also highlights significant differences between the copula and extreme value-based graphs. Notably, the significance of the "Interconnectedness" score, which measures the degree of connections to other banks within the system, is significantly higher in the extreme value-based models. This suggests that these models may be more suitable for extracting linkages between banks. The overall systemic importance score (SIS) is

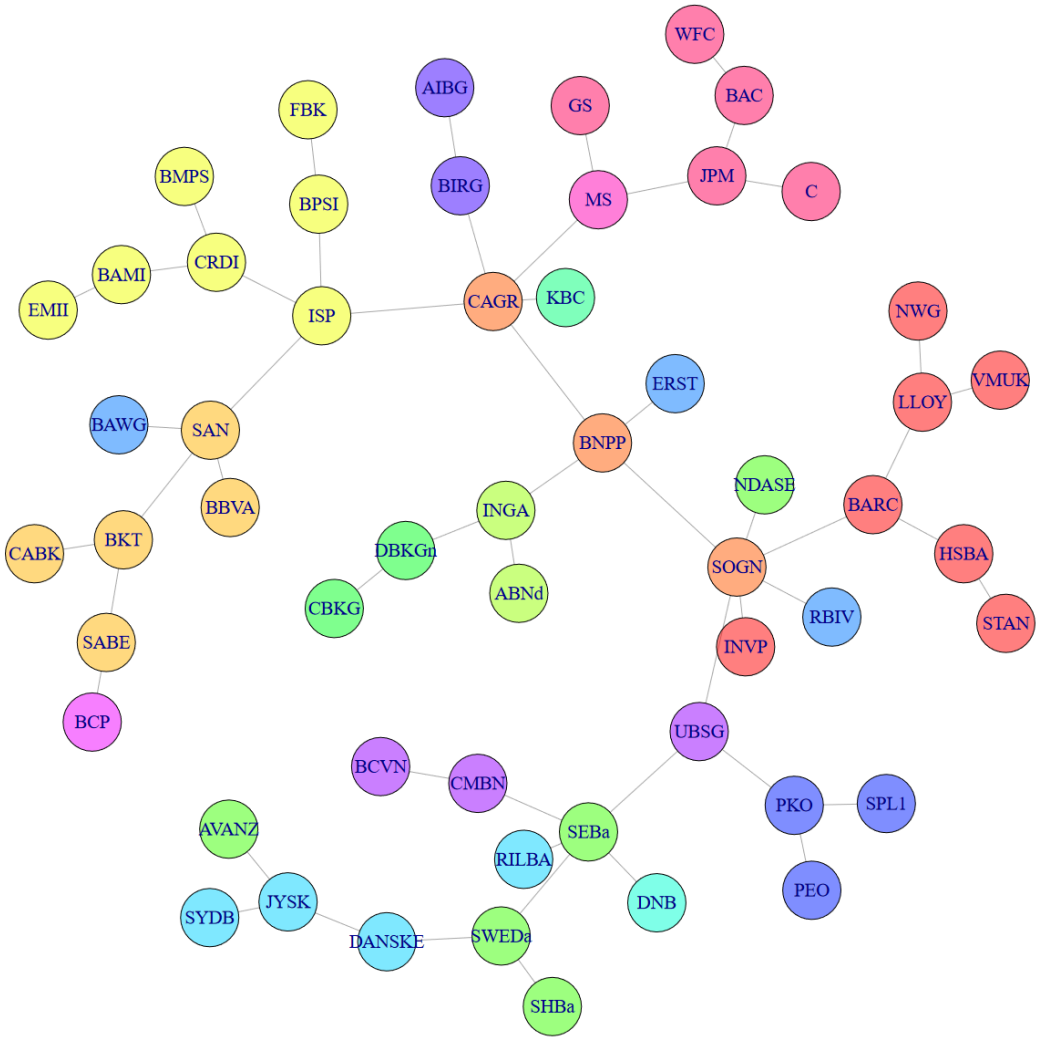

Figure 3: Network structure of European banks based on the extreme value theory approach. Based on last 5 years of data from April 2019 to April 2024. Bank indices are in Appendix Table 5

Table 3: Individual regressions for two OFR G-SIB Scores, Overall score in the SIS and the Interconnectedness score, regressed on closeness, betweenness, and degree centrality measures. The systemic importance score (SIS) is the final score awarded by the OFR and determines the capital requirement add-on, it is based on multiple characteristics including the interconnectedness score. All regressions have n=114 observations and the coefficients are not scaled. ** significant at 1% and * significant at 5%.

	Copula		EVT	
SIS	**Coeff.**	**P-value**	**Coeff.**	**P-value**
Centrality	9534.6	0.207	16464.6	0.065
Betweenness	0.066*	0.020	0.066*	0.022
Degree	6.52	0.062	12.57*	0.013
Interconnectedness				
Centrality	7354.3	0.128	14808.9**	0.009
Betweenness	0.046*	0.012	0.058**	0.001
Degree	4.06	0.069	10.12**	0.002

less significant for both, indicating that graphs alone cannot capture the importance of other key characteristics such as size, substitutability, complexity, or the degree of cross-jurisdictional activity. However, the EVT graphs still outperform the general copula models, remaining more significant across all metrics.

In addition to verifying individual importance and interconnectedness, the centrality measures also allow an even more direct comparison between the Copula and EVT implied graphs. By calculating a monthly rank correlation based on the closeness centrality score we can compare the similarity and dissimilarity over time. As shown in Figure 4, the rank correlation exhibits an upward trend and has increased significantly over the last 20 years. Based on the Dickey-Fuller test the null hypothesis of non-stationarity is not rejected at 5%, however, when adding a drift term the null hypothesis is rejected and the unit root is deemed not present. There is however a statistically significant drift.

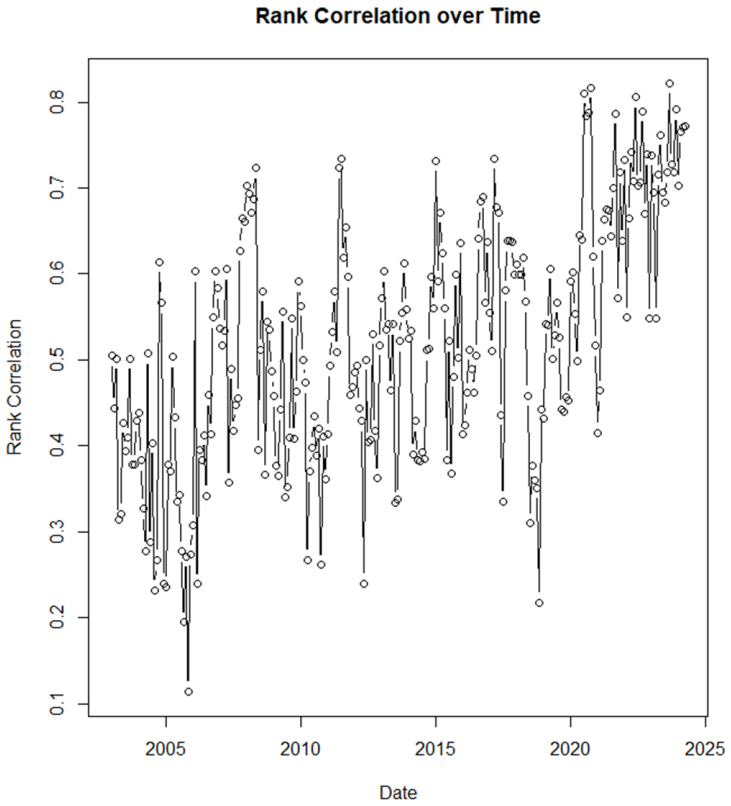

Figure 4: Rank correlation of closeness centrality between copula and extreme value-based trees, based on a three-year moving window.

The F-tests (see Appendix Figure 11) identify three moments where a structural break may have occurred in the data. The first peak was at the Brexit announcement, the second in the middle of the Brexit negotiations, and the third during the Covid pandemic. Overall, this aligns well with the observation that the dependence structure of the banking network in Europe changed significantly around these moments. Notably, in the second series of F-tests, which included the GDP or FSI variable, only the second point remained

significant.

To further investigate this structural break, two subsets around the Brexit negotiations are selected, examining the five years before and the five years after March 2017. This division allows us to assess the impact of Brexit on interbank relationships. The graphs presented in Appendix Figures 17 and 18 for the extremal graphs, and Figures 12 and 13 for the copula-derived graphs, show clear differences. In the extremal graphs the clear movement of Virgin Money and Investec from the centre before Brexit to the outsides of the graph post Brexit is seen. Similarly, while linking to Poland pre-Brexit, the remainder of UK banks now links to the American banks, Nordic banks and a Swiss bank post-Brexit. Signalling a move away from the more central European banks. While the Copula-derived graphs also present a move from the centre for Investec, it is this time joined by Standard Chartered and HSBC. Again a new UK cluster is created towards the outside, but this time it does not link to any other clusters at all. Note that this country specific clustering is in itself also more prominent in copula-graphs regardless.

Besides Brexit, it could be argued that the heightened volatility during the pandemic and the subsequent active markets may have resulted in the structural break. For example, the increase in market activity may have led to more extreme stock movements, causing the copula-based tree to resemble the structure of the extremal tree without Brexit impact as extreme observations become more important in fitting the copula.

Nevertheless, we can also describe the changes in the rank correlation using economic indicators. Namely, Table 4 shows the regressions of the rank correlation on the quarterly GDP of the European Union, the Financial Stress Index (FSI), and the European subset of the FSI. Also a multiple regression with both economic growth and the FSI was performed. Notably, each regression includes the time as an independent variable to adjust for the trend. The results also hold for 5-year time periods, apart from the GDP-growth (most likely due to the length of the period).

As seen, the quarterly GDP is significant with a p-value of 0.0324, suggesting that during periods of high economic growth, the rank correlation decreases. This is logical, as bear markets often feature relatively more extreme observations, allowing extremal graphs to share more similarities with copula-based graphs. Similarly, high FSI numbers are significant at the 1% level for both the entire index and the European-Japanese Subset. The positive coefficient indicates that higher financial stress levels lead to a higher correlation between extremal and copula graphs. This aligns with the previous conclusion drawn from the GDP effect, indicating that economic slowdowns result in higher correlation across the graphs. Notably, neither sign flips in the multiple regression, with GDP remaining significant at the 5% level.

The difference between the copula-based and extreme value theory-based models is further emphasized when considering different measures for the copula model. As shown in Appendix A, the copula model can be utilized with a tail-dependence measure. However,

Table 4: Regressions for the rank correlation between the closeness centrality measures of the copula and extreme value-based graphs. The first regression uses the seasonally adjusted quarterly GDP growth for the European Union. The second and third regressions use measures of financial stress provided by the OFR, specifically the general Financial Stress Index (FSI) and the European-Japan shared Financial Stress Index (EU-JP). All regressions include a constant and a time variable to capture the trend. Note: FSI and EU-JP coefficients are scaled by 100, and the time coefficients are scaled by 10,000. ** indicates significance at the 1% level and * indicates significance at the 5% level.

	Regression 1		**Regression 2**		**Regression 3**		**Regression 4**	
	Coeff	P-value	Coeff	P-value	Coeff	P-value	Coeff	P-value
n	64		181		181		64	
Intercept	-0.77		-9.72		-8.89		-0.71	
GDP	-1.57*	0.034	-		-		-1.60*	0.032
FSI	-		0.77**	0.000	-		0.48	0.222
EU-JP	-		-		1.51**	0.001	-	
Time	0.33**	0.000	0.39**	0.000	0.39**	0.000	0.33**	0.000

the resulting rank correlation between the tail and full measures remains one throughout the period, as depicted in Appendix Figure 7, highlighting that the differences in the graphs stems from the model itself. More explicitly, the measure-dependent difference is non-existent in the current application of the full copula model. This implies that the relationship between a tail-measure-based copula model and the extremal model is identical to that of the full-measure copula model and the extremal model.

6 Conclusion

In conclusion, to find the optimal model to aid regulatory design and model systemic risk through the links within banks, the copula model and extremal model have been thoroughly compared. Differences have been highlighted in graphs and an event study around Brexit has shown the descriptive power of using graphing frameworks. However, the real value lies in the explanatory power of the models.

Here, the new extreme value-based graphs are found to be better at identifying the positions of banks within the system, yielding more significant results when testing capital surcharges and interconnectedness scores across banks. Moreover, the models are also sometimes very similar. This is driven by economic crises and periods of stress, where the rank correlation between the models is found to be dependent on system stress. Finally, when compared to a copula-based tail model, the tail-based modelling approach is found to be superior. Namely, the tail-measure-based copula models do not show any improvement over their full-model counterparts in graphing applications.

Moreover, the results indicate that interbank risk relations are best modelled using tail-specific models opposed to their full model counterparts. This finding is in line with the general assumption that bank failures and other significant risk events are tail-events.

This is particularly important as prior research has highlighted the limited use of market data in determining banking relations, suggesting a potentially significant benefit from incorporating extremal models in future Basel regulations.

The key limitations of the research include the sample size, with the extremal model selecting just a subset of the data, which can be relatively small in the rolling windows. Moreover, the panel of banks is not complete and could include more banks. For Basel regulations, it would need to also include at least the American and Chinese banks, if not a much larger portion of the international banking system. Despite this, the models serve as a successful initial expedition into extremal models, yielding promising results.

Lastly, for the conceptual relationship between using full or tail-specific measures, the copula-based models used are not optimal. Potentially, different, more complex copulas could be tested, or an alternative full model could be considered to create another tail measure for comparison. Nevertheless, the initial results yield significant grounds for further exploration and the potential deployment of extremal models in estimating banking risks and relations.

References

Allahrakha, M., Glasserman, P. & Young, H. P. (2015). *Systemic importance indicators for 33 us bank holding companies: an overview of recent data.* Office of Financial Research.

Baumöhl, E., Bouri, E., Hoang, T.-H.-V., Shahzad, S. J. H. & Výrost, T. (2022). Measuring systemic risk in the global banking sector: A cross-quantilogram network approach. *Economic Modelling*, *109*, 105775. Retrieved from https://www.sciencedirect.com/science/article/pii/S0264999322000219 doi: https://doi.org/10.1016/j.econmod.2022.105775

Bollerslev, T., Chou, R. Y. & Kroner, K. F. (1992). Arch modeling in finance: A review of the theory and empirical evidence. *Journal of Econometrics*, *52*(1), 5-59. Retrieved from https://www.sciencedirect.com/science/article/pii/030440769290064X doi: https://doi.org/10.1016/0304-4076(92)90064-X

Busch, P., Cappelletti, G., Marincas, V., Meller, B. & Wildmann, N. (2021). *How useful is market information for the identification of g-sibs?* (ECB Occasional Paper No. 260). Frankfurt a. M.. Retrieved from https://hdl.handle.net/10419/246191 doi: 10.2866/33823

Calmès, C. & Théoret, R. (2014). Bank systemic risk and macroeconomic shocks: Canadian and u.s. evidence. *Journal of Banking & Finance*, *40*, 388-402. Retrieved from https://www.sciencedirect.com/science/article/pii/S0378426613004603 doi: https://doi.org/10.1016/j.jbankfin.2013.11.039

Carmassi, J. & Herring, R. (2016). The corporate complexity of global systemically important banks. *Journal of Financial Services Research*, *49*, 175–201.

Cerchiello, P. & Giudici, P. (2016). Conditional graphical models for systemic risk estimation. *Expert Systems with Applications*, *43*, 165-174. Retrieved from https://www.sciencedirect.com/science/article/pii/S0957417415006041 doi: https://doi.org/10.1016/j.eswa.2015.08.047

Childers. (2024). *Nonstationary and Persistent Time Series.* https://donskerclass.github.io/EconometricsII/TimeSeriesNonstationarity.html. (73-374 Econometrics II)

Coles, S., Heffernan, J. & Tawn, J. (1999). Dependence measures for extreme value analyses. *Extremes*, *2*, 339-365. doi: 10.1023/A:1009963131610

Coletti, P. (2016). Comparing minimum spanning trees of the italian stock market using returns and volumes. *Physica A: Statistical Mechanics and its Applications*, *463*, 246-261. Retrieved from https://www.sciencedirect.com/science/article/pii/S0378437116304605 doi: https://doi.org/10.1016/j.physa.2016.07.029

Denkowska, A. & Wanat, S. (2020). A tail dependence-based mst and their topological indicators in modeling systemic risk in the european insurance sector.

Risks, *8*(2). Retrieved from https://www.mdpi.com/2227-9091/8/2/39 doi: 10.3390/risks8020039

Embrechts, P., Lindskog, F. & McNeil, A. (2001). Modeling dependence with copulas and applications to risk management. In S. Rachev (Ed.), *Handbook of heavy tailed distributions in finance* (p. 329-384). Elsevier.

Engelke, S. & Hitz, A. (2020, 06). Graphical models for extremes. *Journal of the Royal Statistical Society: Series B (Statistical Methodology)*, *82*. doi: 10.1111/rssb.12355

Engelke, S. & Volgushev, S. (2022, 11). Structure learning for extremal tree models. *Journal of the Royal Statistical Society: Series B (Statistical Methodology)*, *84*. doi: 10.1111/rssb.12556

Engle, R., Jondeau, E. & Rockinger, M. (2014, 03). Systemic risk in europe. *Review of Finance*, *19*(1), 145-190. Retrieved from https://doi.org/10.1093/rof/rfu012 doi: 10.1093/rof/rfu012

Eurostat. (2024). *Eurostat Databrowser.* https://ec.europa.eu/eurostat/databrowser/view/namq_10_gdp__custom_11248570/default/table?lang=en. (Accessed on 10/05/2024)

Farris, J. S., Kluge, A. G. & Eckardt, M. J. (1970). A numerical approach to phylogenetic systematics. *Systematic Zoology*, *19*(2), 172–189. Retrieved 2024-06-26, from http://www.jstor.org/stable/2412452

Freeman, L. C. (1978). Centrality in social networks conceptual clarification. *Social Networks*, *1*(3), 215-239. Retrieved from https://www.sciencedirect.com/science/article/pii/0378873378900217 doi: https://doi.org/10.1016/0378-8733(78)90021-7

Hallac, D., Park, Y., Boyd, S. & Leskovec, J. (2017). Network inference via the time-varying graphical lasso. In (pp. 205–213). New York, NY, USA: Association for Computing Machinery. Retrieved from https://doi.org/10.1145/3097983.3098037 doi: 10.1145/3097983.3098037

Hansen, B. E. (1994). Autoregressive conditional density estimation. *International Economic Review*, *35*(3), 705–730. Retrieved 2024-04-15, from http://www.jstor.org/stable/2527081

Heinen, A. & Valdesogo, A. (2020). Spearman rank correlation of the bivariate student t and scale mixtures of normal distributions. *Journal of Multivariate Analysis*, *179*, 104650. Retrieved from https://www.sciencedirect.com/science/article/pii/S0047259X20302311 doi: https://doi.org/10.1016/j.jmva.2020.104650

Huang, W.-Q., Zhuang, X.-T. & Yao, S. (2009). A network analysis of the chinese stock market. *Physica A: Statistical Mechanics and its Applications*, *388*(14), 2956-2964. Retrieved from https://www.sciencedirect.com/science/article/pii/S0378437109002519 doi: https://doi.org/10.1016/j.physa.2009.03.028

Hüsler, J. & Reiss, R.-D. (1989). Maxima of normal random vectors: between inde-

pendence and complete dependence. *Statistics & Probability Letters*, *7*, 283-286. Retrieved from https://api.semanticscholar.org/CorpusID:222250816

Li, W., Bao, R., Harimoto, K., Chen, D., Xu, J. & Su, Q. (2021). Modeling the stock relation with graph network for overnight stock movement prediction. In *Proceedings of the twenty-ninth international conference on international joint conferences on artificial intelligence* (pp. 4541–4547).

Millington, T. & Niranjan, M. (2021). Construction of minimum spanning trees from financial returns using rank correlation. *Physica A: Statistical Mechanics and its Applications*, *566*, 125605. Retrieved from https://www.sciencedirect.com/science/article/pii/S0378437120309031 doi: https://doi.org/10.1016/j.physa.2020.125605

Monin, P. J. (2019). The ofr financial stress index. *Risks*, *7*(1), 25.

Office of Financial Research. (2024). *G-SIBs G-SIB Scores Interactive Chart.* https://www.financialresearch.gov/bank-systemic-risk-monitor/discontinued-interactive-chart/g-sib-scores-interactive-chart/. (This monitor has been discontinued. The Bank Systemic Risk Monitor has replaced the G-SIB Scores Interactive Chart as of January 2020. The OFR will not update the data provided here.)

Prim, R. C. (1957). Shortest connection networks and some generalizations. *The Bell System Technical Journal*, *36*(6), 1389-1401. doi: 10.1002/j.1538-7305.1957.tb01515.x

Ribatet, M. & Mohammed, S. (2013, 01). Extreme value copulas and max-stable processes. *Journal de la Société Française de Statistique*, *154*.

Rootzen, H. & Tajvidi, N. (2006). Multivariate generalized pareto distributions. *Bernoulli*, *12*(5), 917–930. Retrieved from https://doi.org/10.3150/bj/1161614952 doi: 10.3150/bj/1161614952

Rosas, G. (2006). Bagehot or bailout? an analysis of government responses to banking crises. *American Journal of Political Science*, *50*(1), 175-191. Retrieved from https://onlinelibrary.wiley.com/doi/abs/10.1111/j.1540-5907.2006.00177.x doi: https://doi.org/10.1111/j.1540-5907.2006.00177.x

Rubio, M. & Carrasco-Gallego, J. A. (2016). The new financial regulation in basel iii and monetary policy: A macroprudential approach. *Journal of Financial Stability*, *26*, 294–305.

Schich, S. & Toader, O. (2017). To be or not to be a g-sib: Does it matter? *Journal of Financial Management, Markets and Institutions, Rivista semestrale on line*(2/2017), 169–192. Retrieved from https://www.rivisteweb.it/doi/10.12831/88826 doi: 10.12831/88826

Stiglitz, J. (2009). A bank bailout that works. *The Nation*, *5*.

Tomeczek, A. F. (2022). A minimum spanning tree analysis of the polish stock market.

Journal of Economics and Management, *44*(1), 420–445. Retrieved from https://doi.org/10.22367/jem.2022.44.17 doi: 10.22367/jem.2022.44.17

van Oordt, M. & Zhou, C. (2019). Systemic risk and bank business models. *Journal of Applied Econometrics*, *34*(3), 365-384. Retrieved from https://onlinelibrary.wiley.com/doi/abs/10.1002/jae.2666 doi: https://doi.org/10.1002/jae.2666

Wang, G.-J., Xie, C., Zhang, P., Han, F. & Chen, S. (2014, 05). Dynamics of foreign exchange networks: A time-varying copula approach. *Discrete Dynamics in Nature and Society*, *2014*, 11 pages. doi: 10.1155/2014/170921

Yang, J. & Peng, J. (2020). Estimating time-varying graphical models. *Journal of Computational and Graphical Statistics*, *29*(1), 191–202. doi: 10.1080/10618600.2019.1647848

Yin, X., Yan, D., Almudaifer, A., Yan, S. & Zhou, Y. (2021). Forecasting stock prices using stock correlation graph: A graph convolutional network approach. In *2021 international joint conference on neural networks (ijcnn)* (pp. 1–8).

Zeileis, A., Kleiber, C., Krämer, W. & Hornik, K. (2003). Testing and dating of structural changes in practice. *Computational Statistics & Data Analysis*, *44*(1-2), 109–123. doi: 10.1016/S0167-9473(03)00030-6

Zhang, J. & Luo, Y. (2017). Degree centrality, betweenness centrality, and closeness centrality in social network. *2017 2nd International Conference on Modelling, Simulation and Applied Mathematics (MSAM2017)*, 300–303.

Zhang, Z., Zhang, D., Wu, F. & Ji, Q. (2021). Systemic risk in the chinese financial system: A copula-based network approach. *International Journal of Finance & Economics*, *26*(2), 2044-2063. Retrieved from https://doi.org/10.1002/ijfe.1892 doi: 10.1002/ijfe.1892

Zhou, C. (2010, December). Are banks too big to fail? measuring systemic importance of financial institutions. *International Journal of Central Banking*, *6*(34), 205-250. Retrieved from https://ideas.repec.org/a/ijc/ijcjou/y2010q4a10.html

A Tail Measure Copula Model

The intermediary option between having the full copula model and a tail model is to use the full copula model in combination with a tail-specific measure. For various copulas, there are explicit definitions for tail dependence. In this research, we use the Frank copula and the Gumbel copula, which have the following tail dependences:

$$\lambda_U = \begin{cases} 0 & \text{(Frank)} \\ 2 - 2^{1/\theta} & \text{(Gumbel)} \end{cases} \tag{26}$$

Because of the 0 tail dependence of the Frank copula, we cannot use it to create any graphs. Moving on, for the Gumbel copula, we find that the tail dependence, similar to the explicit relation for Spearman's rho (Equation 27), has a monotonic relationship with its copula parameter θ. This is further highlighted in Figure 5, showing the similar shape.

$$\rho_{Spearman} = 1 - \frac{1}{\theta} \tag{27}$$

Identical results are found across other copulas with direct relationships between the parameters and the measure. Equation 28 shows the relationships for the Student T Copula with copula parameter r and degrees of freedom ν. The tail dependence is from Embrechts, Lindskog and McNeil (2001) and the Spearman's rho relationship is derived by Heinen and Valdesogo (2020) for some mixing density $f_V(\nu)$ for the random variable V. Note that for Spearman's Rho, a simplification to the Gaussian relation ($\rho = \frac{6}{\pi} \arcsin\left(\frac{r}{2}\right)$) can be used, which does not significantly affect the interpretation in the current application (Heinen & Valdesogo, 2020).

$$\lambda_U = 2\left(1 - t_{\nu+1}\left(\frac{\sqrt{\nu+1}\sqrt{1-r}}{\sqrt{1+r}}\right)\right), \quad \rho_{Spearman} = \frac{6}{\pi}\mathbb{E}_V \arcsin(rV) \tag{28}$$

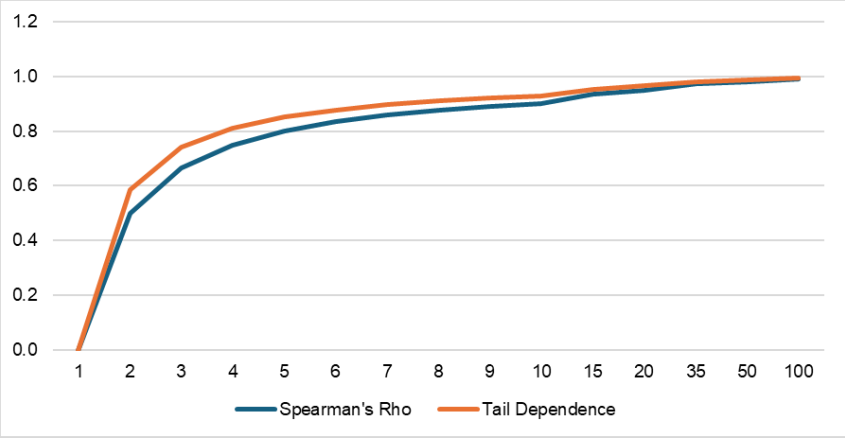

Figure 5: Plot of tail dependence and Spearman's rho against the θ parameter for the Gumbel copula. Note that θ is not to scale.

Because of the monotonic relation shared between the measures (e.g., see Figures 5 and 6), the rank correlation of the assigned edge weights is identical. For example, the relationship between ING and ABN Amro might have a copula parameter of 4. As long as the copula parameter of ABN Amro and BNP Paribas is higher than 4, the lower weight will be assigned to the edge between ABN Amro and BNP Paribas, regardless of which measure is chosen.

More explicitly, since the ranking of the weights remains unchanged across measures, Prim's algorithm creates the same graphs as it iteratively adds the lowest weight edge. Overall, this implies that while the assigned weights may differ across the measures, the resulting graphs will be the same.

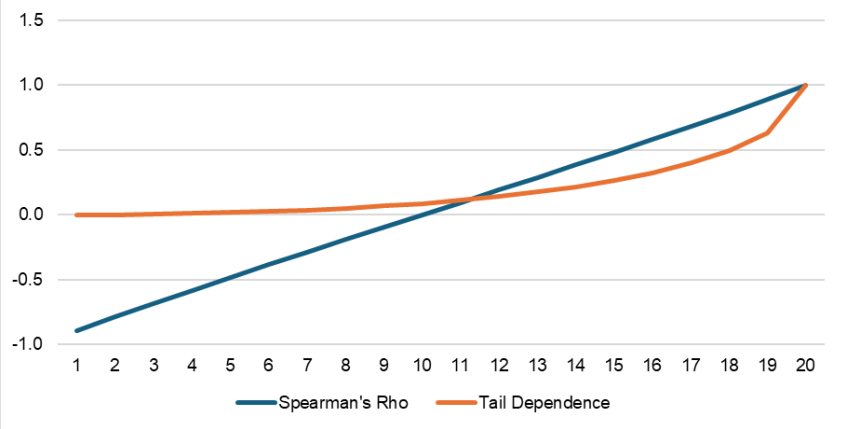

Figure 6: Plot of tail dependence and Spearman's rho against the r parameter for correlation for the T-copula. Under the simplification to the Gaussian formula for Spearman's rho.

The results, as expected, show a rank correlation equal to 1 throughout the period when comparing different measures for the same copula (see Figure 7). This suggests that the increased performance in the tail-tail model stems from the difference in modelling method in the extremal graphs, rather than the change in measure that can be achieved within the full model.

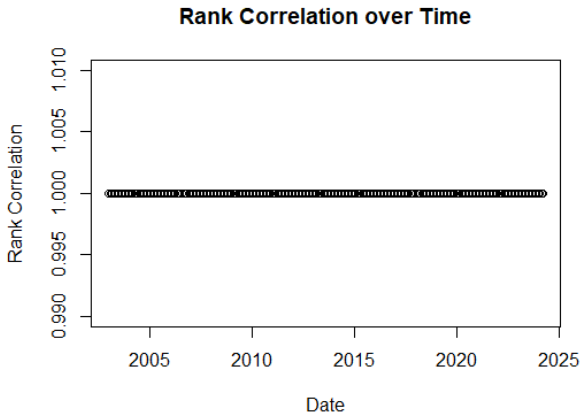

Figure 7: Plot of the rank correlation of the centrality scores between the tail measure and full measure copula-based graphs, shown for the betweenness centrality for the T-copula. Identical graphs can be shown for the Gumbel copula across all centrality measures as well.

B Bank Overview

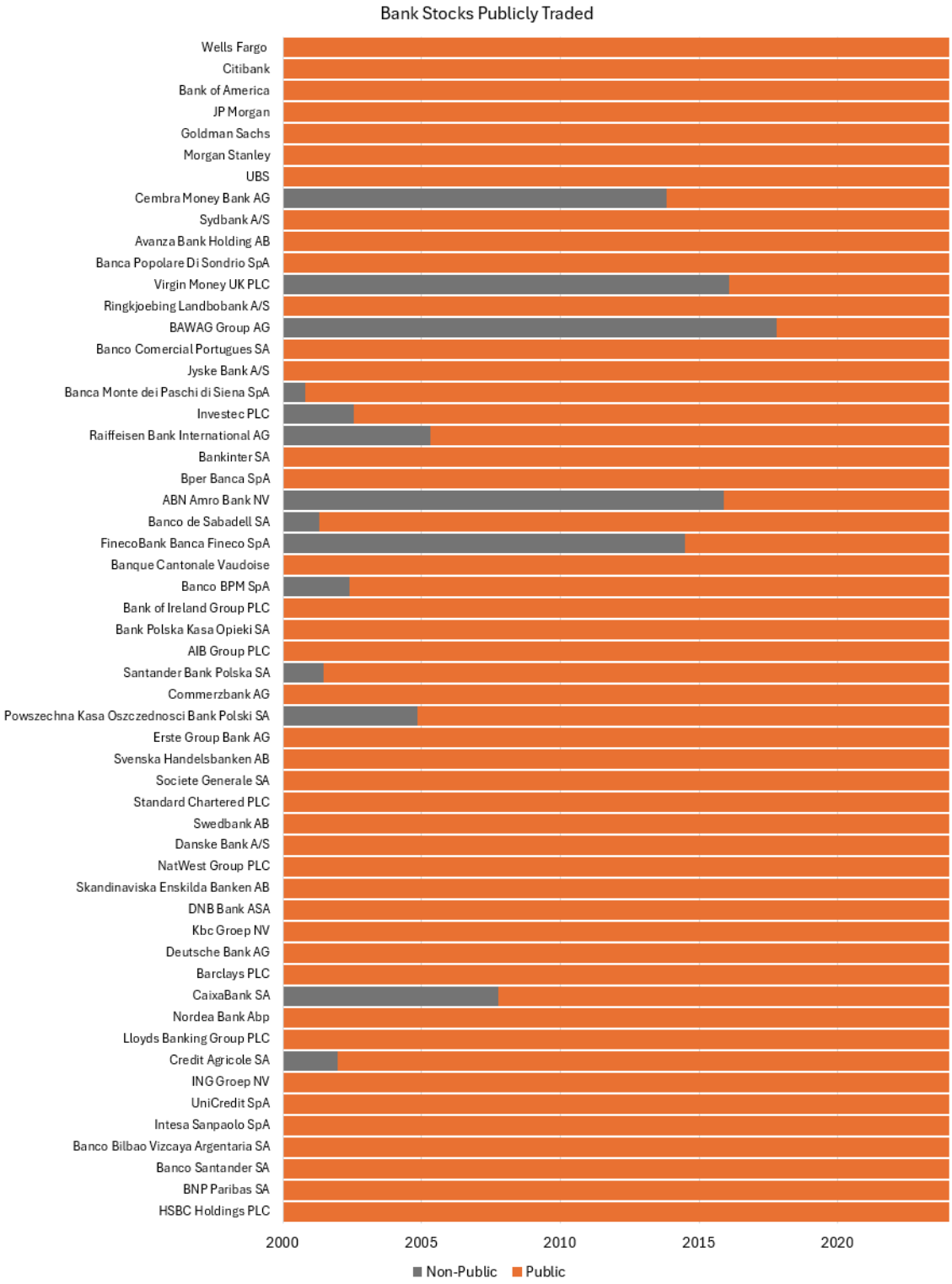

Figure 8: Timeline of trading status for included banks from 2000 to 2024Q1. The plot shows the respective initial public offerings where banks become publicly traded (orange) after private periods (gray).

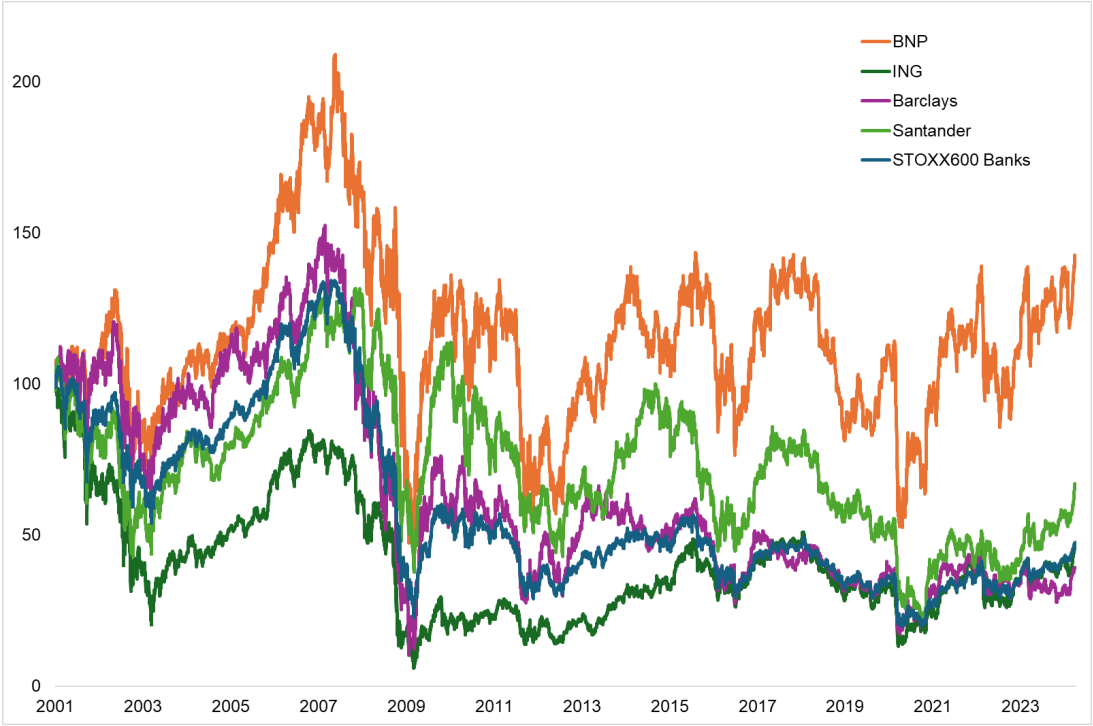

Figure 9: Returns for BNP Paribas, ING, Barclays, Santander and the STOXX600 Banks Index. Rebased to 100 for 01/01/2001 showing the price movements of the period up to 24/3/2024

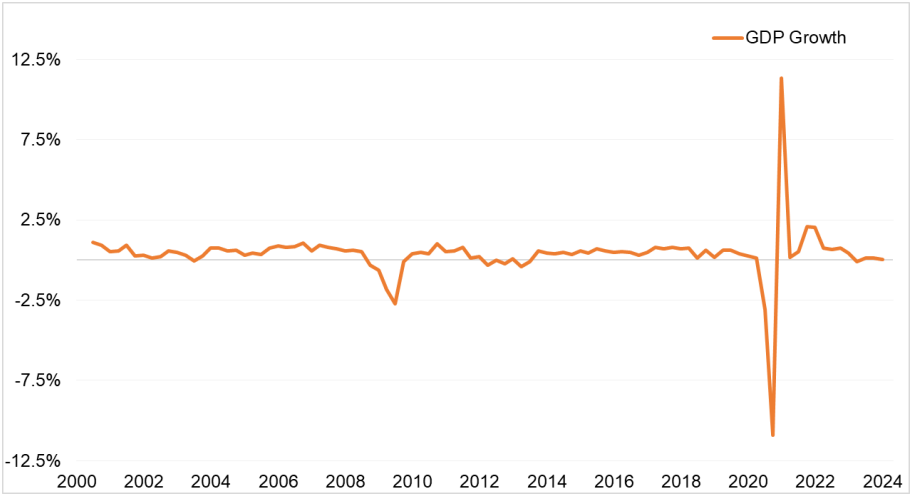

Figure 10: Plot of quarterly GDP growth for European Union. The data is seasonally adjusted and shows the period 2000 to 2024.

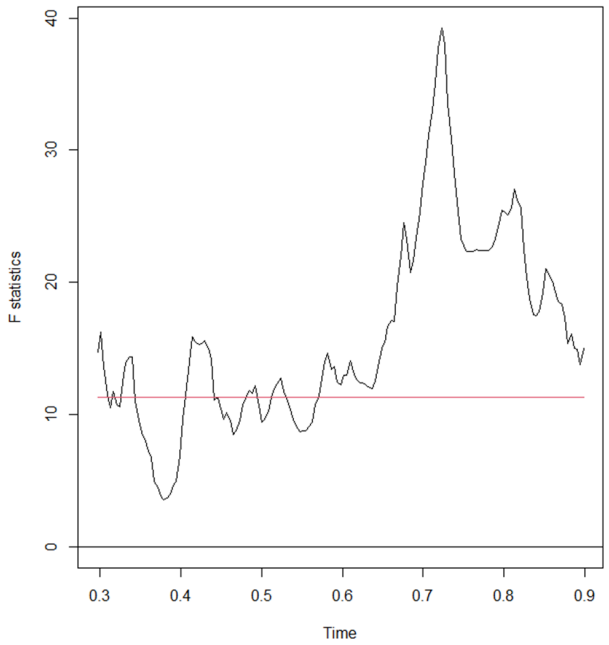

Figure 11: F-test based on a three-year moving window, with the red line indicating the 5% significance level. The subsequent F-tests test for structural breaks in the rank correlation between the copula and EVT based model between 2002 and 2024Q1

Table 5: Description of European banks in the sample with their respective indices. Showing market capitalization and revenue for each bank in €Bn. All banks are members of the European STOXX600 Banks benchmark.

Name	**RIC**	**Market Cap**	**Revenue**
HSBC Holding	HSBA	137.566	60.546
UBS	BNPP	98.212	53.440
BNP Paribas	BNPP	75.068	41.639
Banco Santander	SAN	71.452	58.533
Banco Bilbao Vizcaya Argentaria	BBVA	64.042	33.286
Intesa Sanpaolo	ISP	61.060	24.560
UniCredit	CRDI	59.117	23.424
ING Groep	INGA	53.648	19.744
Credit Agricole	CAGR	41.984	24.567
Lloyds Banking Group	LLOY	38.641	27.405
Nordea Bank	NDASE	37.212	11.724
CaixaBank	CABK	34.390	15.653
Barclays	BARC	32.420	29.033
Deutsche Bank	DBKGn	29.059	28.868
Kbc Groep	KBC	28.944	4.508
DNB Bank	DNB	28.431	6.930
Skandinaviska Enskilda Banken	SEBa	27.062	6.964
NatWest Group	NWG	27.261	16.958
Danske Bank	DANSKE	23.969	7.553
Swedbank	SWEDa	20.889	5.968
Standard Chartered	STAN	20.706	16.181
Societe Generale	SOGN	19.914	21.493
Svenska Handelsbanken	SHBa	18.591	5.401
Erste Group Bank	ERST	17.628	10.389
Powszechna Kasa Oszczednosci Bank Polski	PKO	17.203	5.288
Commerzbank	CBKG	15.751	11.887
Santander Bank Polska	SPL1	13.582	3.491
AIB Group	AIBG	12.491	4.721
Bank Polska Kasa Opieki	PEO	11.063	3.367
Bank of Ireland Group	BIRG	9.989	4.512
Banco BPM	BAMI	9.446	5.102
Banque Cantonale Vaudoise	BCVN	9.209	1.165
FinecoBank Banca Fineco	FBK	8.289	1.235
Banco de Sabadell	SABE	7.918	6.200
ABN Amro Bank	ABNd	7.757	8.664
Bper Banca	EMII	6.187	5.404
Bankinter	BKT	6.195	2.889
Raiffeisen Bank International	RBIV	6.201	8.894
Investec	INVP	5.799	2.173
Banca Monte dei Paschi di Siena	BMPS	5.206	3.802
Jyske Bank	JYSK	5.021	1.991
Banco Comercial Portugues	BCP	4.746	3.744
BAWAG Group	BAWG	4.582	1.517
Ringkjoebing Landbobank	RILBA	4.487	0.513
Virgin Money UK	VMUK	3.274	1.807
Banca Popolare Di Sondrio	BPSI	3.169	1.486
Avanza Bank Holding	AVANZ	3.119	0.384
Sydbank	SYDB	2.728	0.898
Cembra Money Bank	CMBN	2.311	0.531

C Copula Graphs

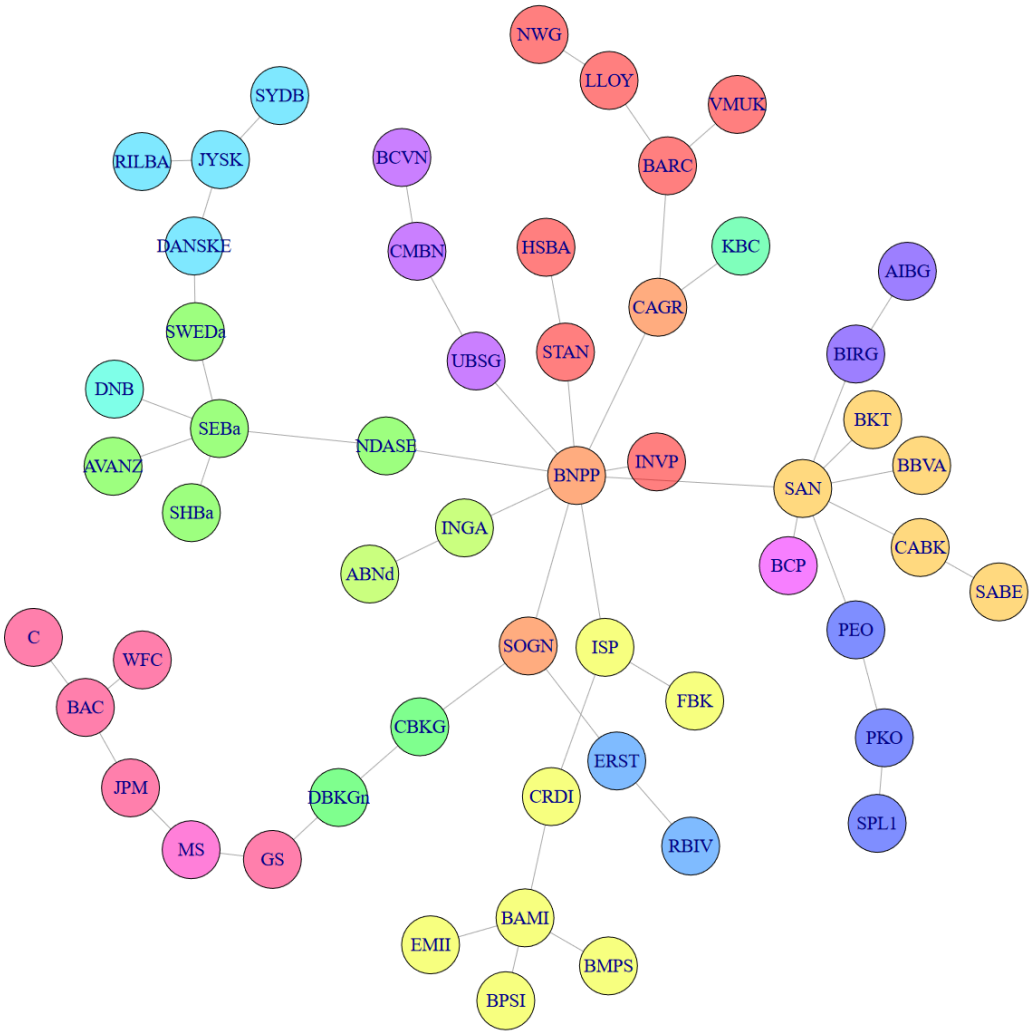

Figure 12: Network structure of European banks based on the Gumbel copula. Based on the 5 years before the Brexit announcement of March 2017. Bank indices are in Appendix Table 5.

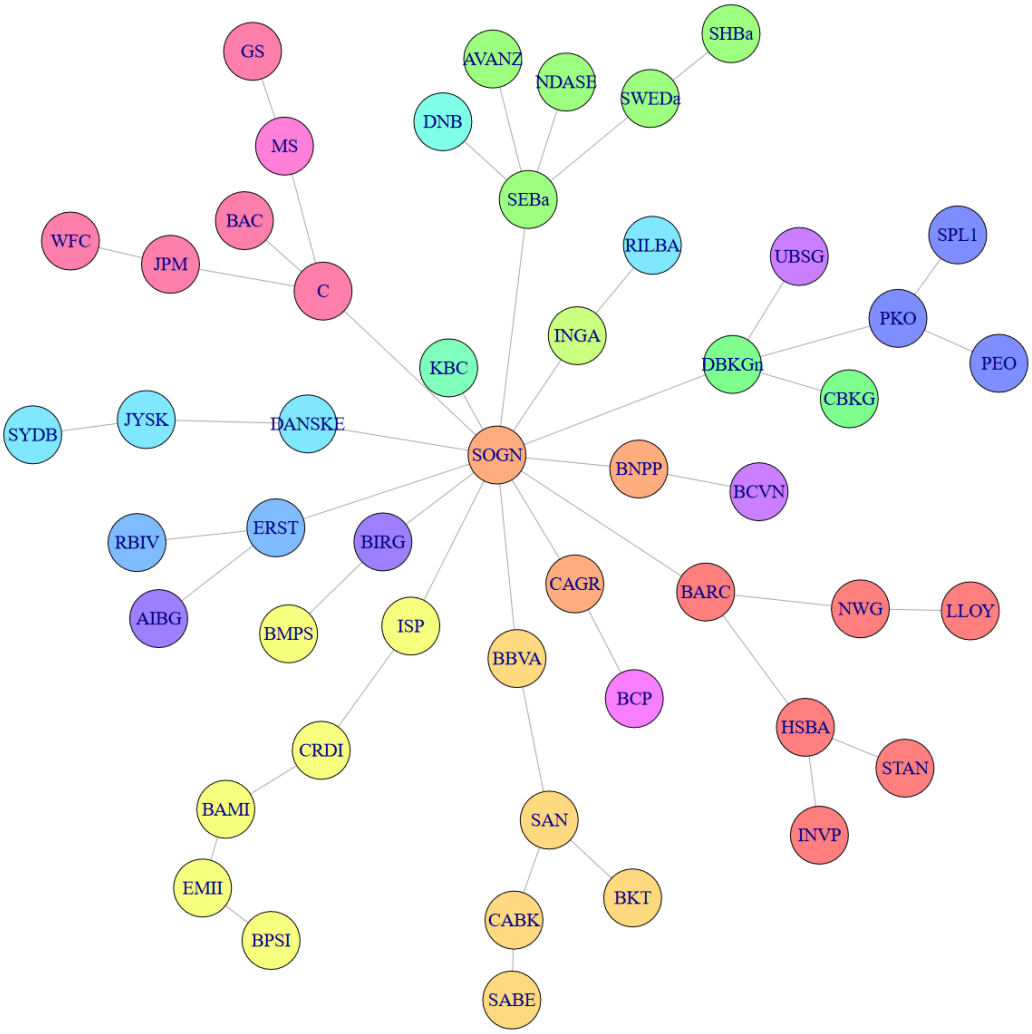

Figure 13: Network structure of European banks based on the Gumbel copula. Based on the 5 years after the Brexit announcement of March 2017. Bank indices are in Appendix Table 5.

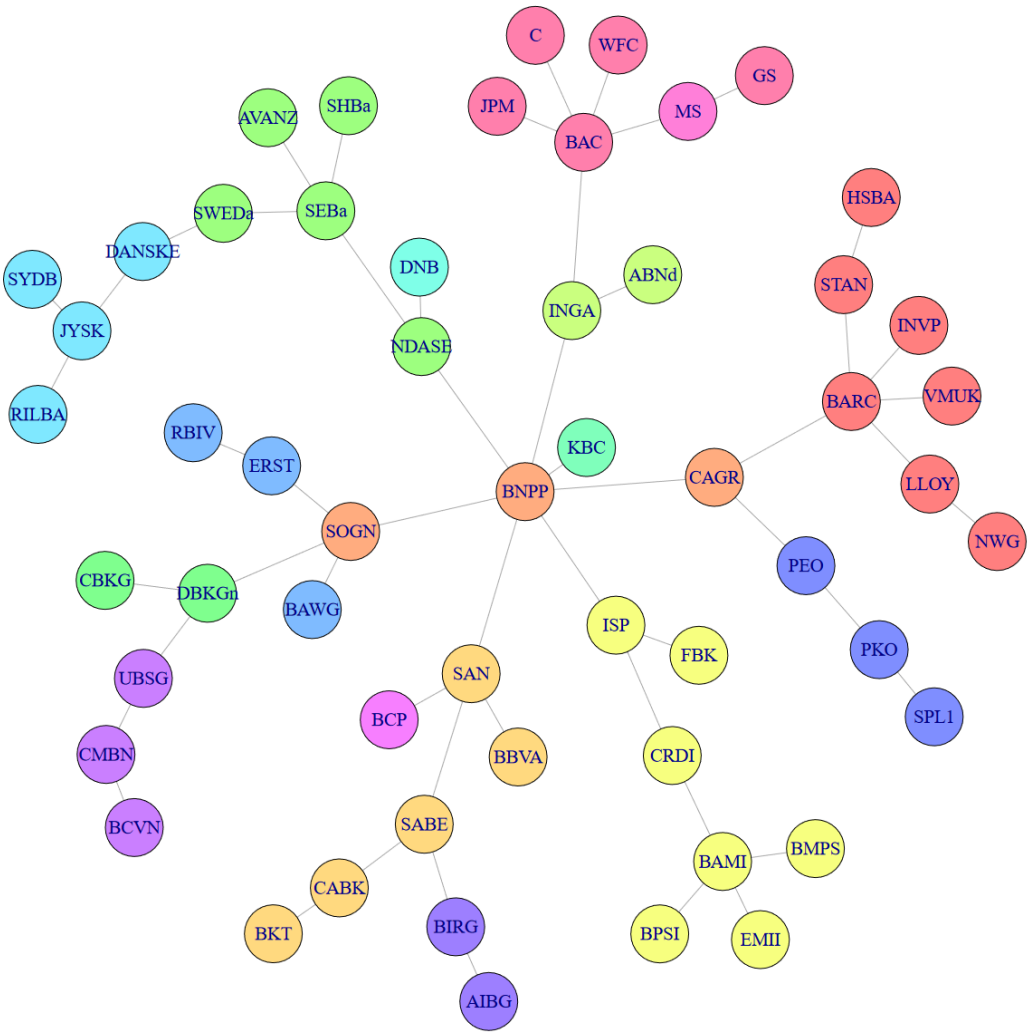

Figure 14: Network structure of European banks based on the Frank copula. Based on last 5 years of data from April 2019 to April 2024. Bank indices are in Appendix Table 5.

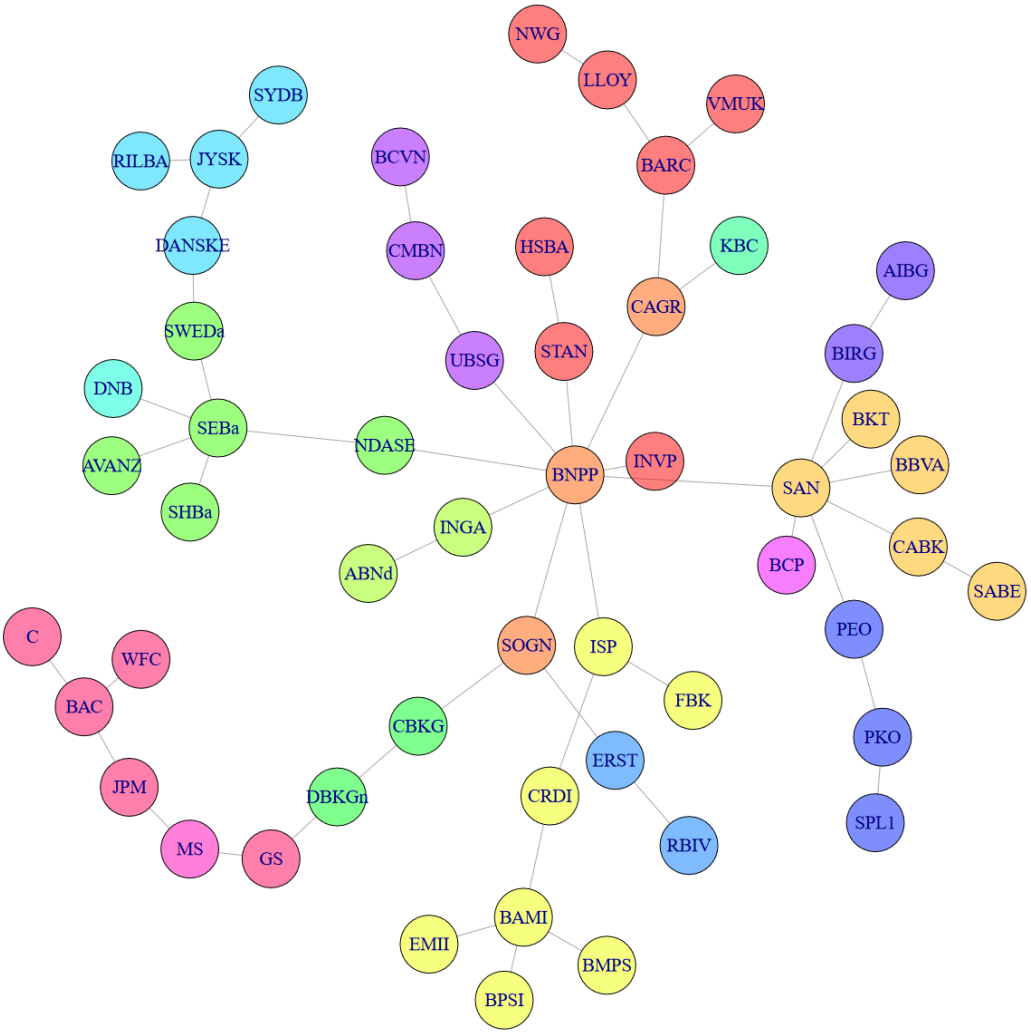

Figure 15: Network structure of European banks based on the Frank copula. Based on the 5 years before the Brexit announcement of March 2017. Bank indices are in Appendix Table 5.

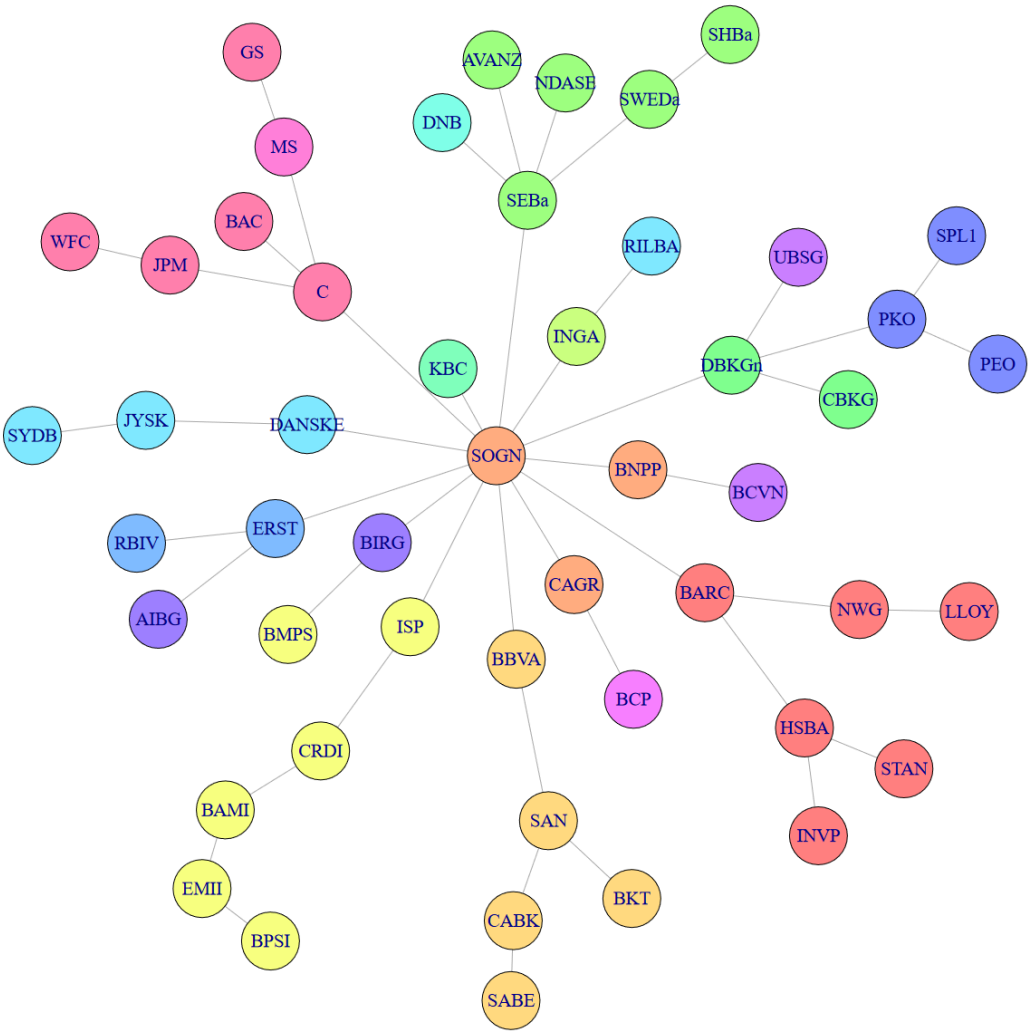

Figure 16: Network structure of European banks based on the Frank copula. Based on the 5 years after the Brexit announcement of March 2017. Bank indices are in Appendix Table 5.

D Extremal Graphs

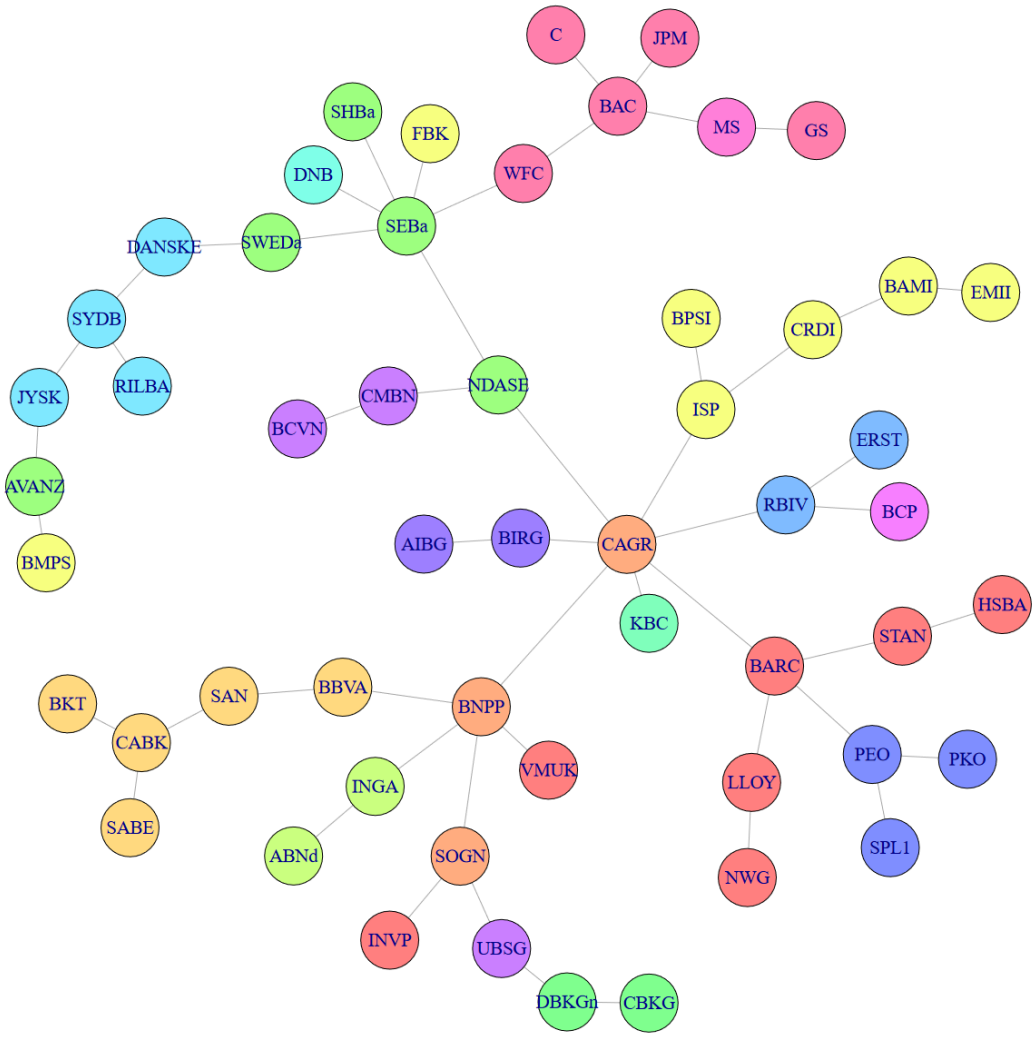

Figure 17: Network structure of banks based on the extreme value theory approach. Showing the 5 years before the Brexit announcement of March 2017. Bank indices are in Appendix Table 5.

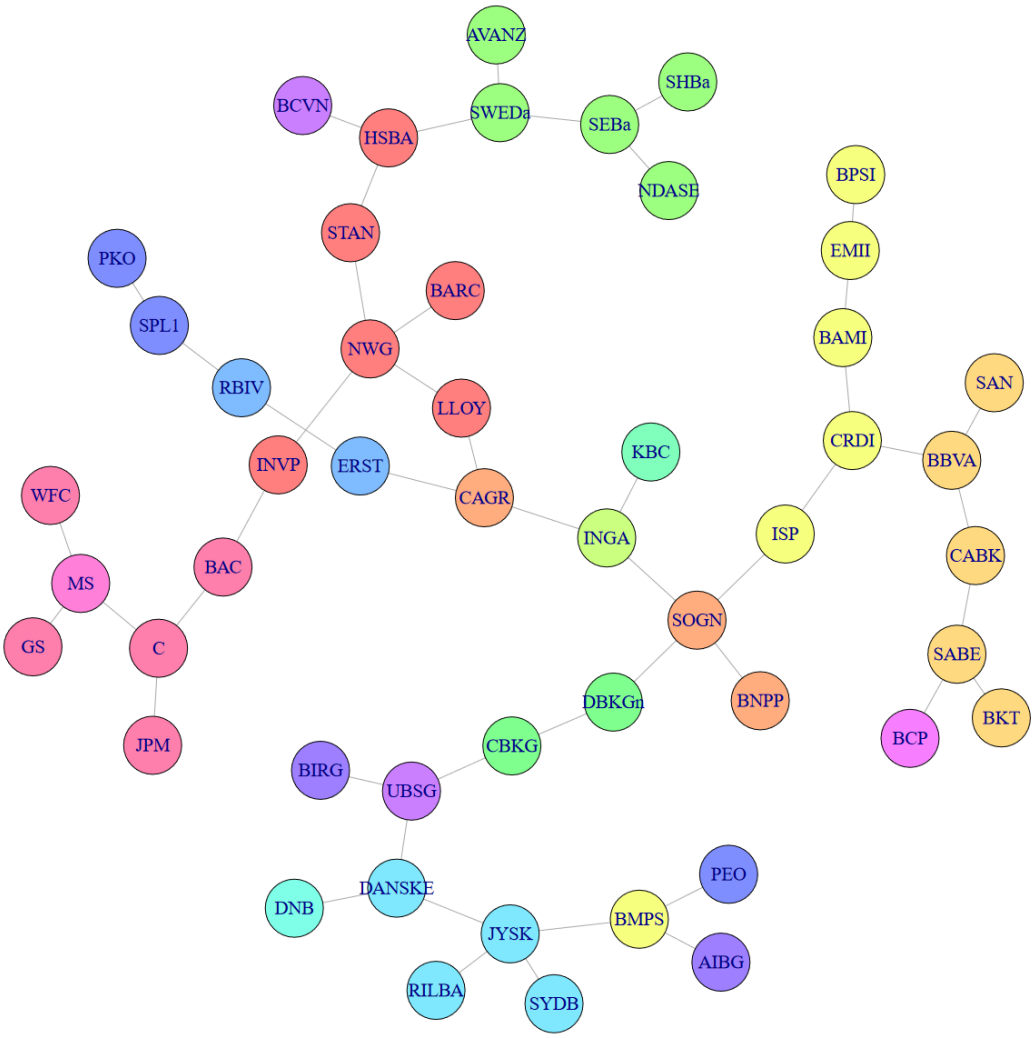

Figure 18: Network structure of banks based on the extreme value theory approach. Showing the 5 years after the Brexit announcement of March 2017. Bank indices are in Appendix Table 5.